

Chitosan/PVA Films and Silver Nanoparticle Impregnated Nanofibrous Dressings for Evaluation of their Wound Healing Efficacy in Wistar Albino Rat Model

SOBHA KOTA*, RATNAKUMARI ANANTHA, VAYUNANDANA RAO GOVADA AND PRADEEP DUMPALA

RVR and JC College of Engineering, Department of Chemical Engineering, Guntur, Andhra Pradesh, India

ABSTRACT

The exoskeleton of marine shrimp contains a natural, biocompatible polymer chitin, which is dumped as a waste. The study proposes the sustainable single-pot-extraction of chitosan from the waste and its use in the fabrication of wound-dressings, and thus leverage its piezoelectric, antioxidant, hypoglycaemic and medicinal properties in wound-healing. The Fourier transform infrared spectrum revealed that marine chitosan contains functional groups with N-O, O-H, and CO stretching. Scanning electron micrographs demonstrated the spherical and mesoporous structures of the extracted chitosan. X-ray diffraction analysis showed a semi-crystalline phase of chitosan particles with a mean size of 28.9 nm. The film prepared with marine shrimp chitosan-polyvinyl alcohol (PVA) composite, and used as a wound dressing exhibited significant wound healing properties with a regeneration efficiency of 78% in 8 days in Wistar albino rats. The wound healing efficiency was enhanced by the addition of cost effective, non-toxic/environmentally friendly silver nanoparticles (AgNPs) synthesized from Rumex acetosa (sorrel) plant extracts and electrospinning of the nanofibrous composites of chitosan/PVA/AgNPs with high antibacterial, antioxidant and wound healing capacity of 96% in 8 days. Thus, the current study supports the use of a natural piezoelectric chitosan polymer as a wound dressing material, either in film or nanofiber, for normal as well as diabetic wounds.

KEYWORDS: *Marine shrimp chitosan, Poly Vinyl alcohol (PVA), Chitosan/PVA composite film, Chitosan/PVA/AgNPs scaffold, Wound healing.*

J. Polym. Mater. Vol. **40**, No. 3-4, 2023, 285-303

© Prints Publications Pvt. Ltd.

*Correspondence author e-mail: sobhakota2005@gmail.com

DOI : <https://doi.org/10.32381/JPM.2023.40.3-4.10>

1. INTRODUCTION

Shrimp processing is one of the largest seafood industries and generates 50%–60% of waste^[1]. In compliance with environmental protection laws and the reuse approach, waste must be utilized in an effective and sustainable manner. Shrimp exoskeleton is abundant in biomaterials and bioactive compounds, including proteins, lipids, minerals, pigments, and a polysaccharide, chitin or poly-(1, 4)-N-acetyl-D-glucosamine^[2]. Due to the increased incidence of surgeries, accidents, burns, and perennial ailments such as diabetes in the 21st century, wound care management has become a challenge. Annually, 76 million people suffer from surgically induced wounds^[3]. The manufacture of suitable non-cytotoxic wound care products with antioxidant and antibacterial properties is necessary. Therefore, attempt was made to synthesize a composite film with chitosan extracted from marine shrimp waste and commercial polyvinyl alcohol and investigated its potential for wound healing in Wistar albino rats. Chitosan or poliglusam is a biodegradable, biocompatible, and innocuous polymer with inherent free-radical foraging (antioxidant) and antimicrobial potential, but is constrained by its poor mechanical strength. To overcome this limitation, chitosan was blended with polyvinyl alcohol (PVA), which is a non-toxic, synthetic, semi-crystalline, biodegradable, cost-effective, and FDA-approved polymer. PVA contains varying numbers of secondary alcohol groups determined by the extent of hydrolysis, which in turn determines the chemical properties, solubility, and crystallinity of the polymer. It easily forms films with high permeation to oxygen and moisture, which are prerequisites for wound healing^[4]. Thus, the composite has

several applications, such as hemostatic and regenerative effects in tissue engineering^[5] and drug delivery systems^[6]. In addition, PVA/Ag-metal-organic frameworks and PVA/chitosan composite hydrogels are used in tissue engineering scaffolds^[7].

Andhra Pradesh, has the third-longest coastline in India (972 km), extending between the Eastern Ghats and the Bay of Bengal. Annually, the shrimp processing industry produces more than 1,50,000 tons of shrimp waste^[8] and dumps as a waste creating environmental threat. From shrimp shell wastes, chitosan can be extracted, and utilized for different applications that include food, biomedical, pharmaceutical, agricultural and chemical industries, and environmental benefits as well; Chitosan/PVA with silver substituted zeolite is used as an active packaging material^[9, 10]. Chitosan alone or in composites has biomedical applications especially in wound healing and a few include Chitosan/PVA/polyhexamethylene guanidine hydrochloride^[11], chitosan hydrogels with extracts from *Aloe vera* and *Calendula officinalis*^[12], chitosan/PVA hydrogel films with honey^[13] in the treatment of periodontal disease^[14], PVA/chitosan loaded with hydroxyapatite and ciprofloxacin^[15] as multifunctional hemostatic sponges. Some of the commercially available chitosan related wound dressing products are Maxiocel, Axiostat, Chitoderm® plus, ChitoSAM™ 100, Celox™, Chitoclear®, Opticell®, ChitoFlex® PRO, ChitoDot®, HemCon® Bandage PRO. Silver™ (Datt Mediproducts Pvt. Ltd, India) is one of the commercially available non adherent, nanocrystalline silver disposable dressing. Research to generate chitosan from discards enhances its availability for industrial use and

concurrently reduces environmental pollution. Chitosan's economical bulk production is warranted and hence, the authors extracted chitosan from shrimp shell waste at a low cost, and evaluated its antioxidant, anti-hyperglycemic effect, and wound healing capacity. Further, the study aimed at the preparation of chitosan/PVA composite film without the use of toxic cross-linking agents, and its efficiency as a wound dressing material was studied in Wistar albino rats. Also, chitosan/PVA nanofibrous scaffolds impregnated with silver nanoparticles (AgNPs) synthesized from *Rumex acetosa* extracts were fabricated by electrospinning and evaluated for their efficacy as wound dressing materials in Wistar albino rats. The in vivo studies revealed a higher antioxidant, antibacterial, and wound healing capacity of electrospun nanofiber scaffold than that of film due to its high porosity, surface area-to-volume ratio, and similarity to the extracellular matrix. Fabrication of the wound dressing nanofibers by the addition of biological AgNPs from *Rumex acetosa* to chitosan/PVA composites enhanced antibacterial and wound healing activities. As chitosan exhibits hypoglycemic activity, it can also be used for the preparation of wound dressings for diabetic patients. A natural piezoelectric chitosan polymer can thus be used as a wound dressing material, either as a film or fibrous scaffold, in normal as well as diabetic wounds.

2. MATERIALS AND METHODS

2.1 Chitosan synthesis from marine shrimp chitin

Chitinous exoskeletal remains of marine shrimp were procured from the Nizampatnam beach of Guntur District, Andhra Pradesh, India (15°54'N, 80°53'E). The

complete extraction process of marine shrimp chitosan was followed as reported by Pradeep et al.^[16].

2.2 Characterization of chitosan

The extracted chitosan was characterized using FTIR, XRD, FESEM coupled with EDX, and TGA. The FT-IR spectrum of chitosan was analyzed from 600 to 4000 cm^{-1} and recorded using a Cary 630 with diamond ATR from Agilent Technologies. The size and crystallinity of chitosan were obtained from the XRD patterns recorded using a Rigaku X-ray diffractometer Ultima IV (2036E202). The morphology and elemental composition of the chitosan sample were investigated using FESEM (Carl Zeiss scanning electron microscope (SEM) with the Oxford EDAX) and EDAX data. Piezoelectric coefficient (d_{33}) was estimated using piezoresponse force microscopy (MFP-3D_BIO V15, Asylum Research, Santa Barbara, CA, USA, and Igor Pro V6). The chitosan/PVA/AgNPs composite nanofibers were characterized by FESEM and EDS, and tested for their tensile strength (INSTRON ID no. 3345R3093, capacity: 5 kN).

2.3 Free radical foraging (anti-oxidant) activity

The ability of marine shrimp chitosan to forage free radicals was assayed using DPPH, FeCl_3 , and ABTS methods. The experimental data collected from triplicates of each test were subjected to statistical analysis. From the regression equation, the IC_{100} was calculated, and an ANOVA was performed.

2.3.1 DPPH assay

Marine shrimp chitosan solutions of 100 $\mu\text{g}/\text{mL}$ to 500 $\mu\text{g}/\text{mL}$ were prepared, and their radical depleting ability was assessed by DPPH assay using the modified protocol of Hsu et al.^[17] To each of the experimental tubes containing a specific concentration of chitosan solution, 2.5 mL of DI water and 1.5 mL of 0.3 mM DPPH in methanol were added and left at room temperature for 30 min. A control, with all the reagents except the sample substance, was set up. Similarly, various concentrations of ascorbic acid from 25 to 125 $\mu\text{g}/\text{mL}$ were set as positive controls. DPPH radical foraging in terms of absorbance was noted with a UV-vis spectrophotometer at 517 nm, and the antioxidant property in percentage was determined using the following equation:

$$\% \text{ Free radical depleting activity (DPPH)} = [(A_c - A_s) /$$

$$A_t] \times 100 \dots (\text{Eq. 1})$$

where A_c and A_t indicate the optical densities of the control and the test/standard respectively.

2.3.2 ABTS assay

Equal quantities of 2.4 mM potassium persulfate and 7 mM 2, 2-azino-bis (3-ethylbenzothiazoline-6-sulfonic acid)(ABTS) were mixed to constitute the stock solution^[18]. The working standard was derived by mixing 1 mL of stock solution with 60 mL of methanol, which has an absorbance of 0.706 ± 0.001 units at 734 nm. To the sets of test tubes containing chitosan (100-500 $\mu\text{g/mL}$) and standard ascorbic acid (25 to 125 $\mu\text{g/mL}$) solution, added 3 mL of ABTS solution and 1 mL of deionized water and kept at room temperature for 20 min. A control was maintained without the sample, and absorbance was measured at 734 nm in a spectrophotometer. The percentage of free radical foraging was estimated by substituting values in Eq. 2.

$$\% \text{ ABTS Inhibition} = \frac{[(\text{Abs of control} - \text{Abs of sample}) / (\text{Abs of control})] \times 100 \dots (\text{Eq. 2})$$

2.3.3 Reducing power assay

Marine shrimp chitosan solutions of increasing concentrations viz. 100 $\mu\text{g/mL}$ to 500 $\mu\text{g/mL}$ were taken in designated test tubes, and their antioxidant potential was estimated following the methodology given by Oyaizu^[19] against ascorbic acid standard in the concentration range of 25 to 125 $\mu\text{g/mL}$. To each reaction tube, added 2.5 mL of 0.2M phosphate buffer (pH 6.6) and 2.5 mL of 1% $\text{K}_3[\text{Fe}(\text{CN})_6]$ and incubated for a duration of 20 min at 50 °C in a hot water bath. Then, added 2.5 mL of 10% TCA (trichloroacetic acid) and centrifuged at 3000rpm for 10min. From this reaction mixture, 2.5 mL of the solution was taken and then added to 0.5 mL of FeCl_3 and 2.5 mL of distilled water. Finally, the OD values were noted at 700 nm, with a blank containing the same reaction mixture components, except for the test sample.

2.4 Hypoglycemic activity of marine shrimp chitosan

The "amylase inhibition" was estimated using the method proposed by Bernfeld^[20], with minor changes. Different concentrations of chitosan viz. 200 to 1000

$\mu\text{g/mL}$ dissolved in 10% acetic acid were added to 1 mL of buffer containing KH_2PO_4 and NaOH (pH 11.0), 1 mL of 1% aqueous starch, 1 mL of human salivary amylase and incubated at 20 °C for a time period of 5 min. Then, all the experimental tubes were added with 2 mL of di-nitro salicylic acid (DNS) reagent, kept in a water bath at 70 °C for 10 min, and then cooled under running tap water. Finally, the brown reduction product obtained in the experimental tubes was added to 10 mL of water, and the OD values were read at 540 nm using a visible spectrophotometer. A blank was prepared with all ingredients except the amylase enzyme. A control was placed without the test sample (marine shrimp chitosan), which represents 100% enzyme activity. A commercial antidiabetic drug, acarbose, in working concentrations of 200, 400, 600, 800, and 1000 $\mu\text{g/mL}$, was used as a positive control. To 1 mL of each of the said acarbose concentrations, 1 mL of 1% starch dissolved in 0.02 M phosphate buffer (pH 6.9) and 1 mL of human salivary amylase were added, followed by incubation at 20 °C for 5 min. This step was succeeded by adding 2 mL of DNS reagent and executing the steps mentioned above for the chitosan sample. The percent inhibition of amylase by chitosan and acarbose is expressed as

$$\% \text{ amylase inhibition} = [(A_c - A_t) / A_c] \times 100 \dots (\text{Eq.3})$$

where A_c and A_t represent the respective absorbance values of the control and test samples.

2.5 Fabrication of the chitosan/PVA composite films

Typically, for the fabrication of the composite films, 500 mg of powdered chitosan was dissolved in 25 mL of 10% acetic acid and was kept with continuous stirring to obtain a homogeneous solution at ambient temperature for 1 day; then 2g of PVA in 30 mL of DI-water and 2 mL of glycerol were added to the solution containing chitosan. Afterwards, this chitosan/PVA solution was left for 6 h to allow air bubbles to escape. The homogenous gel was then transferred into a plastic petri plate of 7 cm diameter and dried at 40 °C in an incubator for 24 hours. The film was peeled out, cut into 5x5 cm dimension, attached to cotton and gauge materials and used as wound dressing.

2.6 Efficacy study of chitosan/PVA composite

film as wound dressing material in vivo in the Wistar albino rat model

Three groups, each comprising five wistar albino rats, in the weight range of 150-180 g were used in the current study. After an acclimation period of one week, the rats were subjected to experimentation. The consultant veterinary doctor anesthetized the rats with a dose of 50 mg of ketamine hydrochloride/kg of body weight of the animal, and a wound by excision with a circular area of 3 x 3 cm² was made using surgical equipment. The control group rats were not given any treatment; the standard group were dressed with a cotton gauge patch containing povidone-iodine solution; and in the test group, the wound was covered with a wound dressing containing marine shrimp chitosan/PVA composite film (vide materials and methods section). The wound dressings were replaced with fresh ones on alternate days, and the readings were noted just before placing the new dressing.

Wound contraction (%) = [(Initial wound area – Specific day wound area) / Initial wound area] X 100.....(Eq. 4)

2.7 Fabrication of the chitosan/PVA/AgNPs composite nanofiber by electrospinning and its efficacy study in vivo in the Wistar albino rat model

Marine chitosan composite nanofibers were prepared by adding 10µg of green synthesized silver nanoparticles (AgNPs)^[21] to the chitosan/PVA solution,

electrospun the scaffolds at a voltage of 15.4 kV and a flow rate of 0.7 mL/hr for 9 hours. The optimum temperature and humidity maintained were 26.7°C and 77% respectively^[22].

3. RESULTS

3.1 Characterization of biomaterials

3.1.1 Characterization of Chitosan

Chitosan extracted from marine shrimp chitin was characterized by several analytical techniques, including FESEM-EDAX, FTIR, X-ray diffraction (XRD), and thermogravimetric analysis, to understand the physicochemical characteristics. SEM coupled with EDAX was used in this analysis, and ten iterations were performed. The SEM morphology shows that the chitosan is spherical with a mesoporous nature (Fig. 1a). From EDAX, the extracted chitosan biopolymer was found to contain carbon to the extent of 69.76%, followed by oxygen (23.46%), nitrogen (3.11%), chlorine (1.8%), sodium (1.38%) and silicon (0.49%) (Fig. 1b).

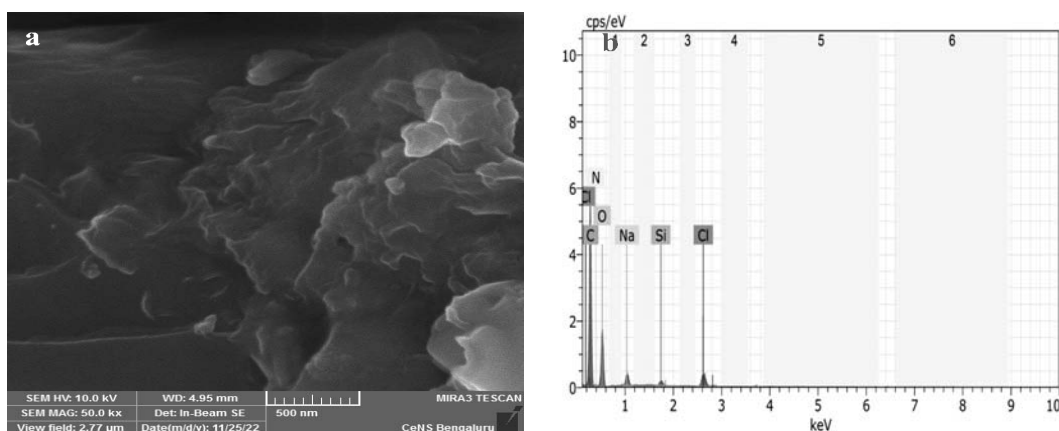


Fig. 1a. FESEM pattern b. EDS spectrum of the extracted marine shrimp chitosan

FTIR spectroscopic analysis revealed prominent spectral bands for the extracted chitosan sample at 50.97, 72.53, 98.05, 892.9, 1149.28, 1376.08, 1322.37, and 3200 to 3400 cm^{-1} (Fig. 2). Of these, the band at 1322 cm^{-1} corresponds to C(O)-O stretching vibrations and OH in plane vibrations, with a slight shift from the standard 1317 cm^{-1} ^[23]. In addition, this band is very close to 1320 cm^{-1} , which is characteristic of Amide III linkages. The spectral band at 1149 cm^{-1} is indicative of C-O stretching vibrations similar to those in the C-O-C glycosidic linkages of oligosaccharides. Furthermore, the spectral bands in the range of 3200-3400 cm^{-1} could be ascribed to O-H stretching vibrations^[24].

The X-ray diffractogram of marine shrimp chitosan revealed intense peaks at 2θ values of 31.4° and 45.16° (Fig. 3), and our results match those reported as 30.5° and 45° for a semi-crystalline chitosan biopolymer^[25]. The other sharp peaks obtained between 45° and 75° are characteristically found in commercial chitosan²⁶. The particle size was calculated using the Scherer equation,

$$D = K\lambda / \beta \cos \theta \dots \quad (\text{Eq. 5})$$

where, λ is taken as (the wavelength of X-ray source) 0.1541 nm, β is the full width at half maximum (FWHM) of the diffraction peak, K is a constant with a value of 0.9 (Scherer constant) and θ is the Bragg's angle; the calculated mean size was 28.9 nm.

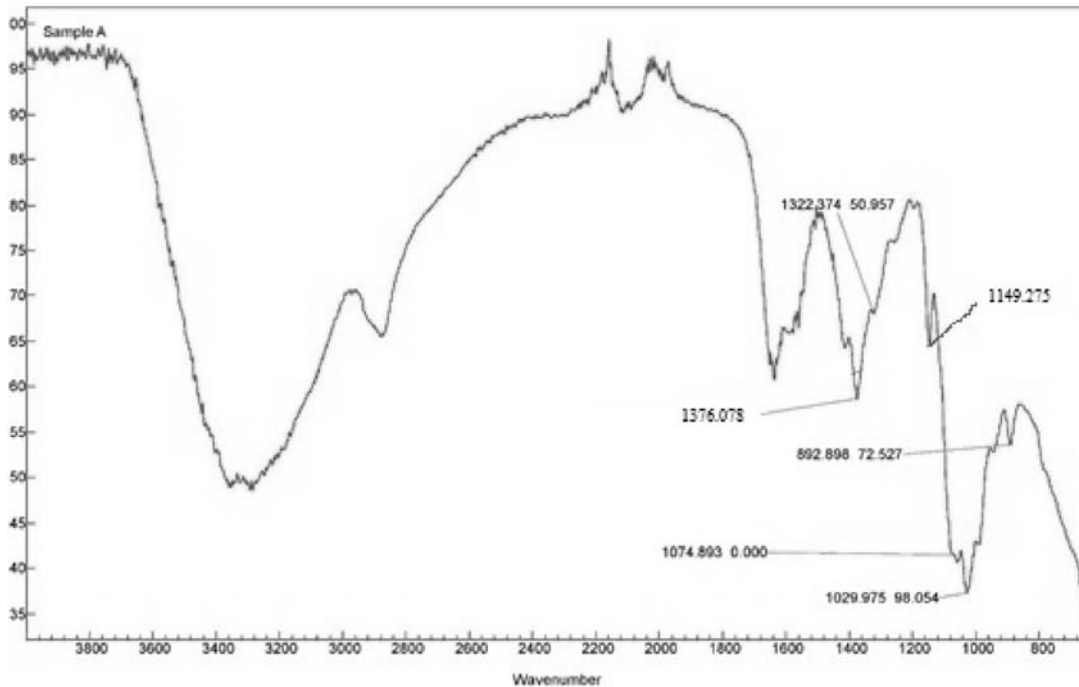


Fig. 2. FTIR spectrum of the extracted marine chitosan sample

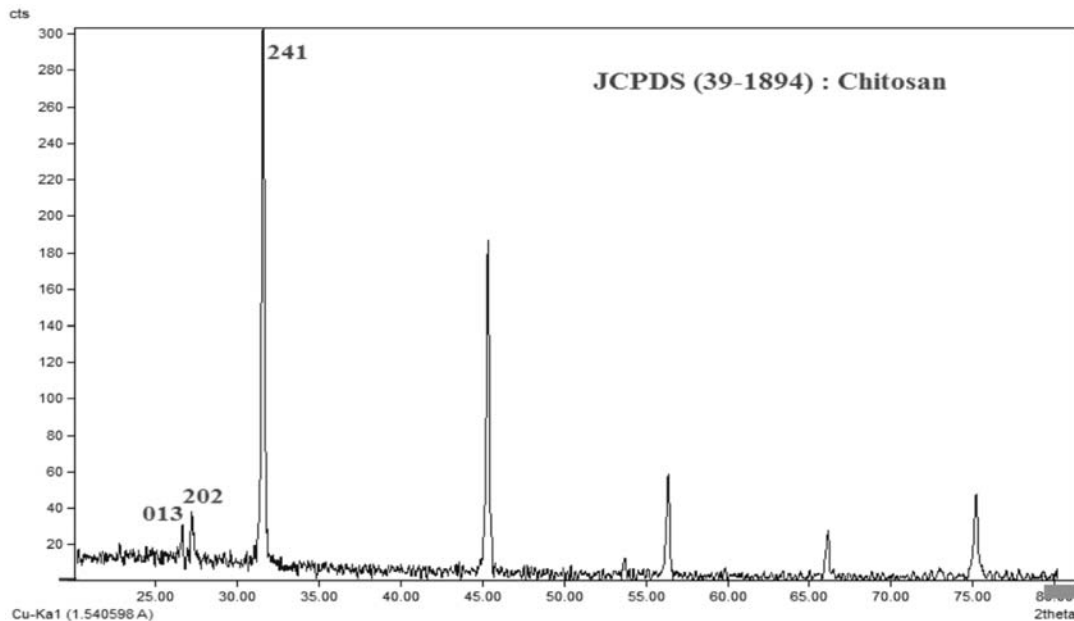


Fig. 3. X-ray diffractogram pattern of the extracted marine chitosan

Piezo response force microscopy (PFM) was performed, and the data obtained was used to determine the local piezoelectric response of the marine shrimp chitosan. The topology of amplitude and phase is as shown in Figs. 4a and 4b, and the PFM with phase and amplitude in response to bias voltage is shown in Fig. 4c. In PFM, a tip was fixed on a single particle, and voltage was applied across the particle, known as bias voltage, and its corresponding structural deformation as an electro-mechanical response was recorded in terms of PFM phase data and amplitude. The phase and amplitude of the PFM data yield the material polarization and local strain responses. PFM evaluates the nanoscale electro-mechanical behavior of the marine chitosan-based single nanoparticle with topography, phase, and amplitude as a function of applied voltage (bias voltage) in between -20

V and +20 V, as shown in Fig. 4c. The phase images in Figs. 4a and 4b display dark and bright regions of the polarization directions, and an interesting observation is the occurrence of a corresponding phase hysteresis loop, which represents a linear phase at 60° in negative bias voltage. The amplitude signal from marine shrimp chitosan interprets the butterfly loop characteristic, which resembles the piezoelectric property. The variation of strain (S) is equal to amplitude response changes under the influence of an electrical field (E); thus the piezoelectric coefficient (d_{33}) of the marine shrimp chitosan can be calculated using the formula $S = d_{33}E$ ^[27-29].

The maximum amplitude for marine chitosan obtained was 110 pm at 20 V and 235 pm at -20 V. Using the above formula, the calculated mean piezoelectric coefficient (d_{33}) is 3.7 pm/V.

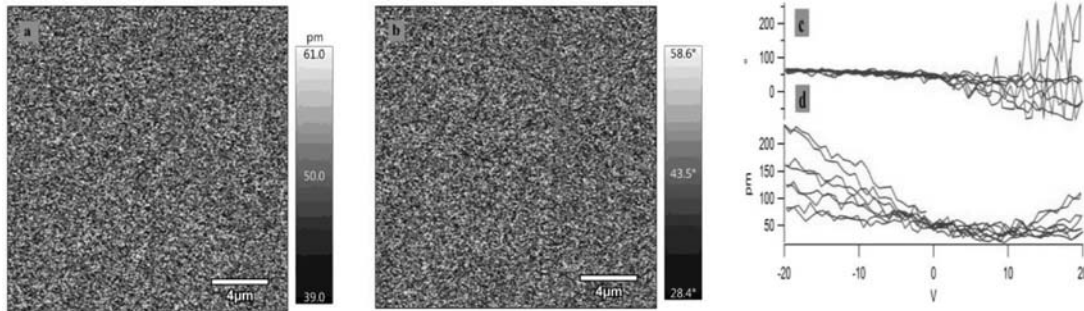


Fig. 4a, 4b, 4c & 4d. Piezoresponse Force Microscopy (PFM) characterization

3.1.2 Chitosan/PVA/AgNPs nanofibers

Chitosan/PVA/AgNPs nanofibers were fabricated using an electrospinning unit (Fig.

5a), and the formed nanofiber is represented in Fig. 5b. The stress-strain curve of Chitosan/PVA/AgNPs nanofibers is shown in Fig. 5c.

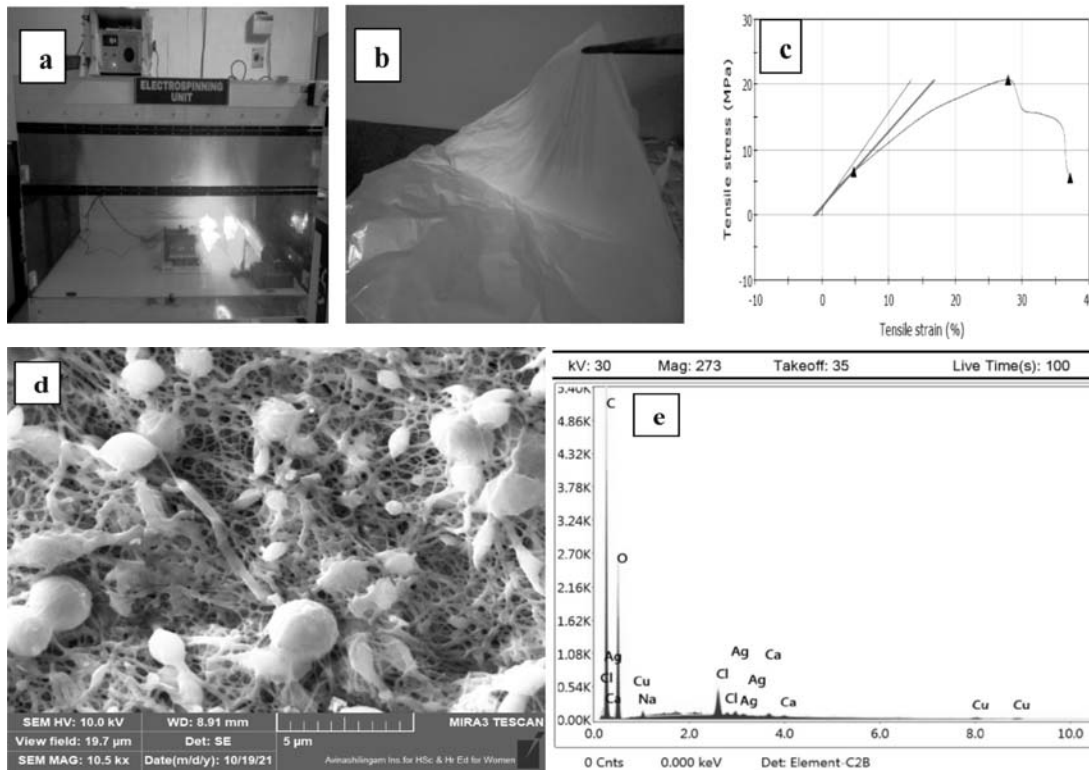


Fig. 5a. Fabrication of nanofibers using electrospinning machine b. Electrospun nanofiber (Chitosan/PVA/AgNPs) c. Tensile strain Vs. Stress analysis d. Scanning electron microscope pattern of electrospun nanofiber e. Energy dispersive spectroscopic peaks denoting the presence of silver nanoparticles in nanofiber.

The mean tensile test properties of load break were 12.27 N, while tensile stress break of 10.22 N/mm², extension break of 27.02 mm, Young's modulus of 215.73 MPa, and a maximum load of 33.21 MPa for tensile stress were obtained. FESEM analysis revealed the fibre diameter of electrospun Chitosan/PVA/AgNPs nanofibres as 240 nm (Fig. 5d). Energy dispersive spectroscopy (EDS) analysis of Chitosan/PVA/AgNPs nanofiber revealed a peak for metallic silver, with the weight compositions for carbon, oxygen, and silver at 61.51%, 37.23%, and 0.05%, respectively. In addition, low-intensity peaks reflecting the presence of some elements, e.g., Na, Cl, and Ca, are evident in the spectrum (Fig. 5e).

3.2 Free radical foraging (Antioxidant) activity

Free radicals, released during metabolic reactions in the body, damage cells and tissues, and hence, antioxidants that can counter them are released by living cells. The dangerous effects of free radicals can be nullified by natural polymers such as chitosan. The antioxidant capacity of chitosan was determined by DPPH, FeCl₃ and ABTS assays and ANOVA results are presented in Table 1.

3.2.1 DPPH Assay

DPPH is the most potent test for determining antioxidant potential. Donation of a hydrogen atom by the antioxidants to the free radicals results in a complex of DPPH₂ and thus decreases the absorption at 517nm. Visually, this is observed as a reduction in the intensity of the purple color, an indication of radical scavenging. The free radical foraging potential of ascorbic acid increased from 65.39 to 96.47% for the tested concentrations.

Chitosan's free radical scavenging activity increased from 7.8 to 12.96% with an increase in concentration from 100 to 500 µg/mL. The IC₁₀₀ values for ascorbic acid and chitosan were respectively 117 µg/mL and 6870 µg/mL (Fig. 6a).

3.2.2 ABTS assay

The change in the color of the experimental solution from deep bluish-green to pale green/colorless indicates the reaction between the antioxidant substance and the ABTS free radical and is directly proportional to the free radical foraging ability. The radical scavenging activity of ascorbic acid increased from 33.48 to 93.39% with an increase in concentration from 25 to 125 µg/mL (Fig. 6b). The scavenging activity of chitosan increased from 7.97% to 42.61% with an increase in concentration from 100 to 500 µg/mL.

3.2.3 FeCl₃ assay for the reduction potential

The reducing potential of marine shrimp chitosan was measured by FeCl₃; the higher the absorbance, the higher the reducing power/antioxidant activity. The ascorbic acid showed an increase in absorbance from 0.286 to 1.418 with an increase in concentration from 25-125 µg/mL, as shown in Fig. 6c; simultaneously, the color of the solution changed from yellow to green. Chitosan showed a very low reducing power ranging from 0.041 – 0.055 with an increase in concentration from 100 to 500 µg/mL.

3.3 Hypoglycemic activity

One of the methods to control hyperglycemia is the inhibition of amylase, which is responsible for the breakdown of starch into maltose (Disaccharide) and glucose

(monosaccharide units). The antidiabetic potential of chitosan was determined by estimating its amylase inhibition effect. Acarbose is a commercial amylase inhibitor and is used as a standard to compare amylase inhibition by chitosan. The percentage inhibition effect of marine shrimp chitosan was compared with that of acarbose (Fig. 6d), and the IC₁₀₀

values are tabulated (Table 1). The % inhibition caused by chitosan and acarbose increased from 15.09 to 63.98% and 78.71 to 96.43%, respectively, with an increase in concentration from 200-1000µg/mL. This suggests that chitosan, if incorporated into medications, can have considerable hypoglycemic effects.

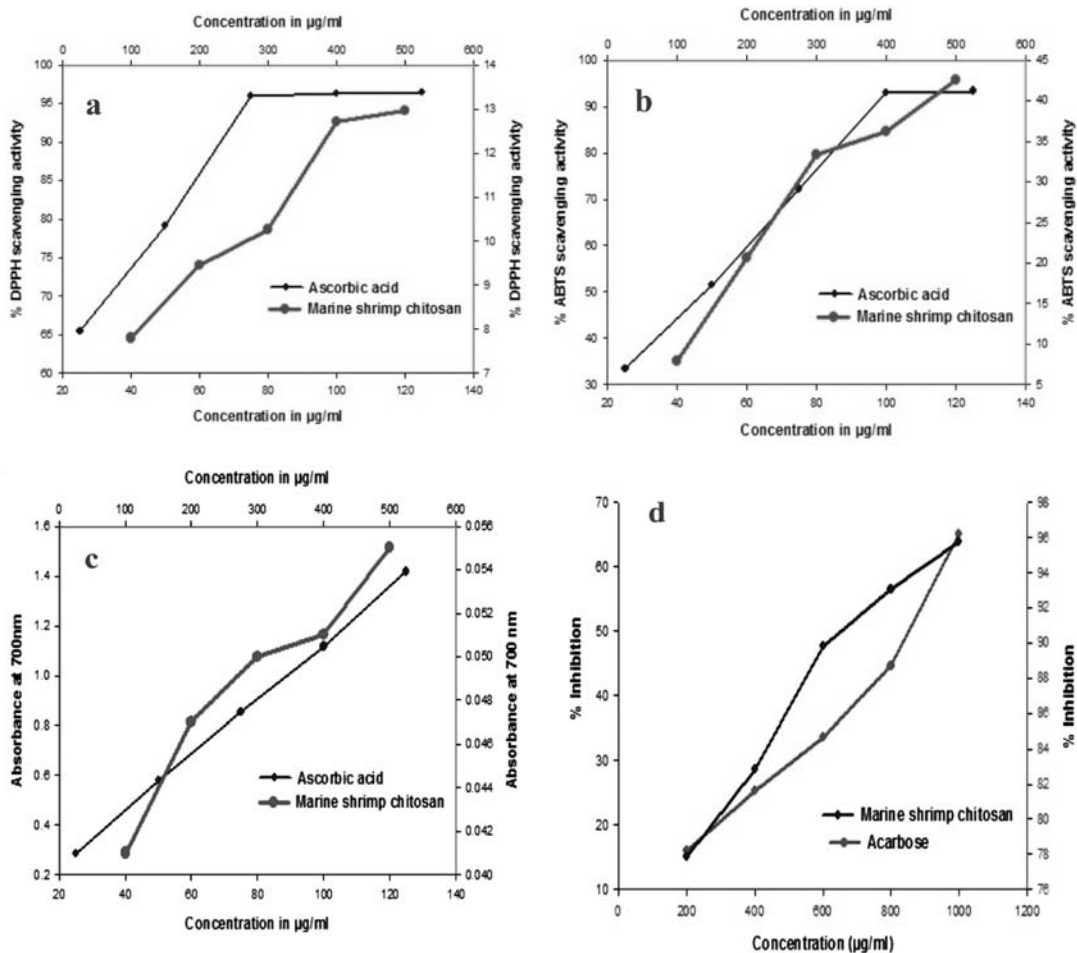


Fig. 6a. DPPH b. ABTS c. Reducing power assays depicting free radical scavenging d. Hypoglycemic activity of marine shrimp chitosan

TABLE 1. One-way Analysis of Variance (ANOVA) for the marine shrimp chitosan antioxidant and hypoglycemic activities tested

Assay	Standard/ test	Regression equation	IC ₁₀₀ Concentration	Results of One way Analysis of Variance (ANOVA)				
				Parameter	Sum of Squares (SS)	Degrees of Freedom (df)	Mean Square (MS)	F value p value
DPPH	Ascorbic acid	y = 0.3172x + 62.84 R ² = 0.8029	117.15	Between groups	14435.44	1	14435.44	143.9
				Within group	802.52	8	100.31	
	Total	15237.96	9	-	0.0000			
ABTS	Ascorbic acid	y = 0.6449x +20.351 R ² = 0.947	123	Between groups	4110.35	1	4110.35	9.3675
				Within group	3510.3	8	438.78	
	Total	7620.65	9	-	0.0155			
FeCl ₃	Ascorbic acid	y = 0.0112x +0.011 R ² = 0.9995	8927	Between groups	1.6088	1	1.6088	16.4063
				Within group	0.7844	8	0.098	
	Total	2.3932	9	-	0.0036			
Antidia- betic activity	Acarbose	y = 0.0215x + 72.945 R ² = 0.9598	1258	Between groups	4724.102	1	4724.102	20.789
				Within group	1817.894	8	227.23	
	Total	6541.996	9	-	0.001			

Note: * indicates a significant difference between the standard and the test sample (P<0.05)

TABLE 2. Percentage of wound healing area in control, standard, and test Wistar albino rats (C: Control; Standard – Iodine-Povidone)

S. No.	Days	Wound area (cm ²)							
		C (cm ²)	Wound healing area (%)	Std. (cm ²)	Wound healing area (%)	Marine chitosan/PVA composite film (cm ²) (cm ²)	Wound healing area (%)	Marine chitosan/PVA/AgNPS nanofibre	Wound healing area (%)
1	0 day	9.0	0	9.0	0	9.0	0	0	0
2	2 day	8.55	5	8.28	9	7.38	18	6.82	23
3	4 day	8.28	8	7.74	14	6.12	32	3.38	62
4	6 day	7.2	20	6.12	32	3.78	58	1.65	81
5	8 day	6.3	30	4.62	48	1.98	78	0.29	96

3.4 Marine shrimp chitosan/PVA composite film wound dressing - the efficacy study

The wound healing area measured on days 2, 4, 6, and 8 in rats that received wound dressings containing marine chitosan/PVA composite films showed significantly high reduction, suggesting a faster healing process because of the inherent property of chitosan. A visual presentation of the data of Table 2 is provided in Fig. 7 for a quick understanding of the differences in the process and time involved in wound healing among the three groups of rats that served as control, standard, and test samples. From the results presented in Table 2, it is evident that the percentage wound healing is high in rats dressed with marine shrimp chitosan/PVA composite film in apposition with the control and the iodine-povidone treatment. Therefore, the chitosan/PVA composite films are suggestive for incorporation into general wound dressings for effective wound care management.

4. DISCUSSION

Chitosan is a cationic polymer with beta 1®4 linkages joining N-acetyl glucosamine and D-glucosamine units. Piezoelectric materials convert mechanical energy into electrical energy. The mechanical energy of body movements provides the electrical stimulation of the natural chitosan component of the fabricated wound dressings. In turn, by virtue of its piezoelectric property, chitosan causes the depolarization and re-organization of local membrane potential. These de- and re-polarizations of the cell membranes trigger the ion channels and effect Ca²⁺ influx, which in turn promotes the gene transcription of cellular factors responsible for cell proliferation and differentiation^[30]. The foraging ability of chitosan is due to the presence of amino and hydroxyl groups that can react with free radicals. The antioxidant activity of chitosan is indirectly related to the mol.wt.^[31]. High-molecular-weight chitosan showed no antioxidant activity, whereas low-molecular-weight chitosan has more amino and hydroxyl groups due to less

*Chitosan/PVA Films and Silver Nanoparticle Impregnated Nanofibrous Dressings for 297
Evaluation of their Wound Healing Efficacy in Wistar Albino Rat Model*

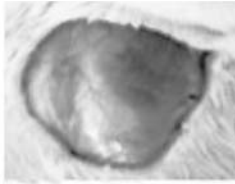
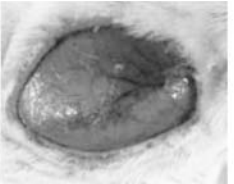
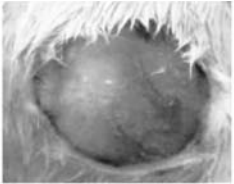
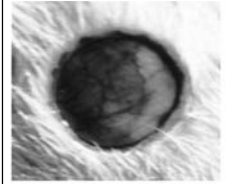
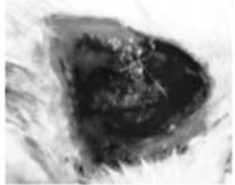
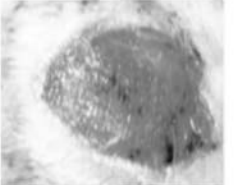
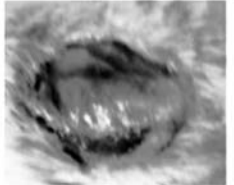
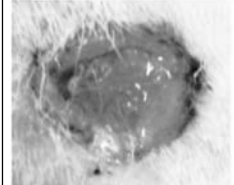
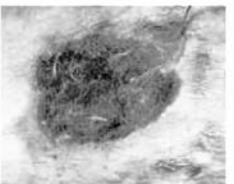
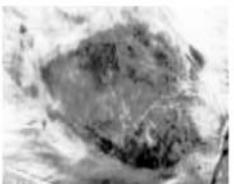
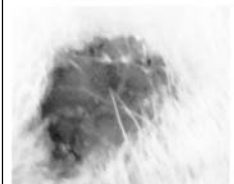
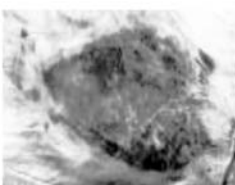
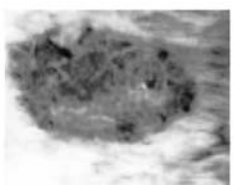
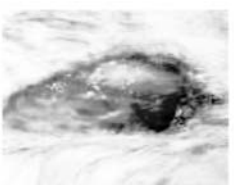
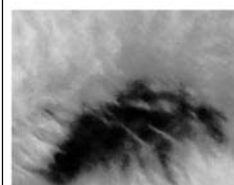
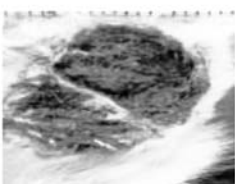
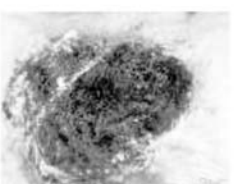
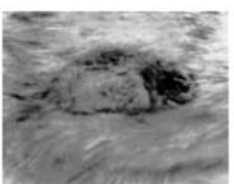
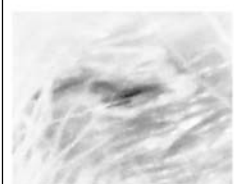
S. No.	Control	Standard (Povidinerodine)	Chitosan/ PVA film	Chitosan/ PVA/AgNPs nanofibre
0 day				
2 day				
4 day				
6 day				
8 day				

Fig. 7. A Comparative wound healing study of control, standard and marine shrimp chitosan/PVA composite film and Chitosan/PVA/AgNPs nanofiber wound dressings on Wistar albino rats.

formation of intramolecular hydroxyl bonds. DPPH[•] radical is remarkably stable and purple in color; it is neutralized by either receiving a 'H' or an e⁻ from chitosan (hydroxyl / amino groups) and converted into a reduced form viz. DPPH or DPPH-H, giving a pale yellow color. The free radical depleting function of chitosan observed in this study ranged between 7.8% and 12.96% because of the occurrence of chitosan in its native form and because of its high molecular weight. The literature states that chitosan at a concentration of 10 mg/mL had only 25.44% antioxidant activity and its IC₅₀ value could not be determined^[32]. The advantages of the DPPH assay are simple, sensitive, reproducible, and efficient with weak antioxidants. ABTS^{•+} radical (unstable and appears blue-green in color), accepts an electron from the chitosan and regenerates ABTS (stable form) and changes into a pale cyan color. The benefits of this assay are that ABTS radicals are cationic, stable, and soluble in both organic and aqueous media. The extracted chitosan exhibited 7.97%-42.61% free radical scavenging activity by ABTS. Reducing potential/antioxidant assay by FeCl₃ is a simple, inexpensive, sensitive, and reproducible technique that involves the reducing potential of transition metal; Fe turns the solution from colorless to intense blue. Liu et al.^[33] studied superoxide, hydroxyl, DPPH, and H₂O₂ scavenging activities. The DPPH scavenging activity of chitosan was 26.11%, whereas the same for N, O carboxymethyl chitosan, and its grafted derivatives of ferulic acid, caffeic acid, and gallic acid were 51.85%, 59.26%, 64.81%, and 74.54%, indicating the lowest activity of chitosan when compared to phenolic acid grafted carboxymethyl chitosan. Phenolic acid-conjugated chitosan exhibited

1.79-5.05, 2.44-4.12, and 1.35-3.35-fold increases in DPPH, H₂O₂, and ABTS radical depletion, respectively, when compared with natural chitosan^[34]. According to Rajoka et al.^[35], the free radicals combine with the free -OH and -NH² groups at C-2, C-3 and C-6 positions of chitosan to form a stable molecule (Fig. 8).

Acarbose is a complex oligosaccharide and an oral amylase inhibitor that reduces glucose absorption in the intestine, and after a meal, the rise in blood glucose levels is checked. Acarbose was chosen as a standard to authenticate the anti-amylase activity of the marine shrimp chitosan. The results demonstrated that chitosan inhibited amylase activity with IC₁₀₀ of 1516 ug/mL, showing its potential as a hypoglycemic agent. Through PI3K/AKT pathway, chitosan shows the anti-hyperglycemic activity. In Diabetes mellitus, the major risk factor is oxidative stress due to which the β-langerhan cells of pancreas are damaged^[36]. According to Karadeniz et al.^[37], chitosan is an antioxidant, protects the β langerhans cells of pancreas, increases the insulin secretion and thus the blood glucose levels are maintained (Fig. 8). Chitosan promotes wound healing and prevents bacterial infection; a literature survey demonstrated that curcumin cross-linked chitosan/polyvinyl alcohol showed wound reduction by 52.33% on the 7th day and 84% on the 14th day^[38]. In contrast, the present marine shrimp chitosan and polyvinyl alcohol composite film showed 78% wound healing in only 8 days; this highlights that chitosan obtained from the marine shrimp chitin is non-toxic, non-allergenic, and offers a sustainable use of

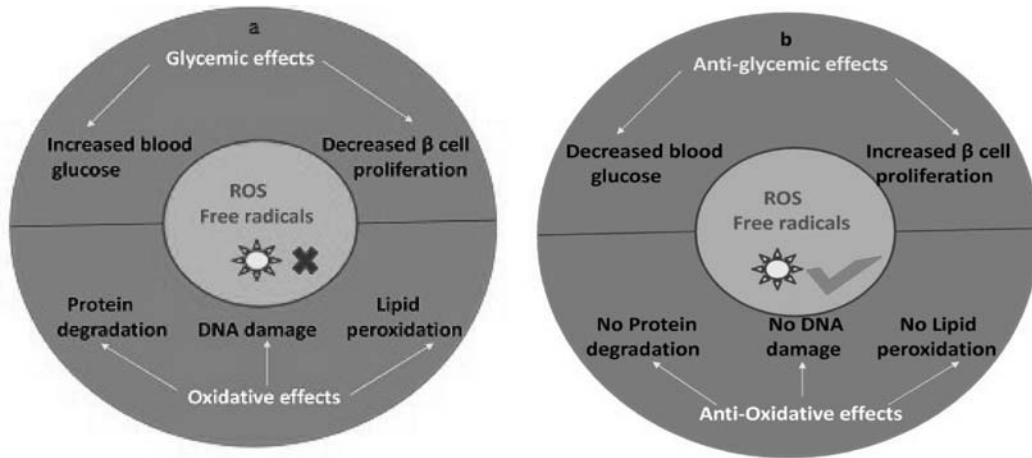


Fig. 8. Oxidation and glyceamic effects in absence (a) and presence (b) of chitosan.

( - Chitosan)

the shrimp exoskeletal wastes. The probable mechanisms involved in wound healing by chitosan-based wound dressings are the enhancement of natural blood clotting, absorption of inflammatory exudates, and provision of a scaffold for cell growth. These properties of chitosan strengthen newly formed tissues and prevent infections by forming a barrier, reduce pain by blocking nerve endings, and even reduce the formation of scar tissue.

In a normal wound-healing process, the first phase is hemostasis, activated by platelets that adhere to the injured endothelium. Platelets and their derived growth factors, together with coagulation factors like fibronectin, fibrin, vitreous connexin, and thrombin, form the blood clot. Within 24-36 hours after injury, neutrophils are the prime cells mobilized to the lesion site in the inflammation phase. Immune cells like macrophages, neutrophils and T lymphocytes gather at the wound site to phagocytose the bacteria and necrotic tissue. During cellular

proliferation, chemical molecules secreted by M2 macrophages modulate cellular neo-vascularization, granular tissue, and re-epithelialization. Fibroblasts play the key role at the wound site as proliferation progresses. The remodeling phase can last from a few weeks to several years. The new skin is formed and completely covered by fibroblasts. TGF and EGF play a vital role in re-epithelialization, angiogenesis, and granular tissue formation. The synthesis of a high-strength collagen matrix is accompanied by the transformation of granular tissue into a mature scar tissue. The new skin is finally formed and completely covered by the fibroblasts.

Chitosan plays a major role in the first three stages of wound healing. Chitosan is positively charged and interacts with the negatively charged molecules on the platelet and erythrocyte surface, promoting the aggregation of platelets and erythrocytes, and inhibits fibrinolysis during hemostasis (Fig. 9a). Chitosan exhibits immunomodulatory

properties: macrophages release pro-inflammatory and anti-inflammatory cytokines during M1 and M2 state respectively^[39]. Low doses of chitosan induce type 1 interferons, leading to increased release of IL-1 receptor antagonist (IL-1 Ra) and CXCL10/IP-10, and low levels of IL-1 β and PGE2. Whereas high doses of chitosan cause increased release of IL-1 β and PGE2 and low levels of IL-1 Ra and CXCL10/IP-10 (Fig. 9b). During proliferation,

chitosan promotes the growth of granulation tissue and finally the skin is remodeled (Fig. 9c, d).

Chitosan/PVA/AgNPs electrospun nanofiber scaffold demonstrated 96% wound healing capacity in Wistar albino rats due to its porous nature and high surface area-to-volume ratio (Fig. 7). AgNPs, due to their unique physical and chemical properties at nano-level, showed

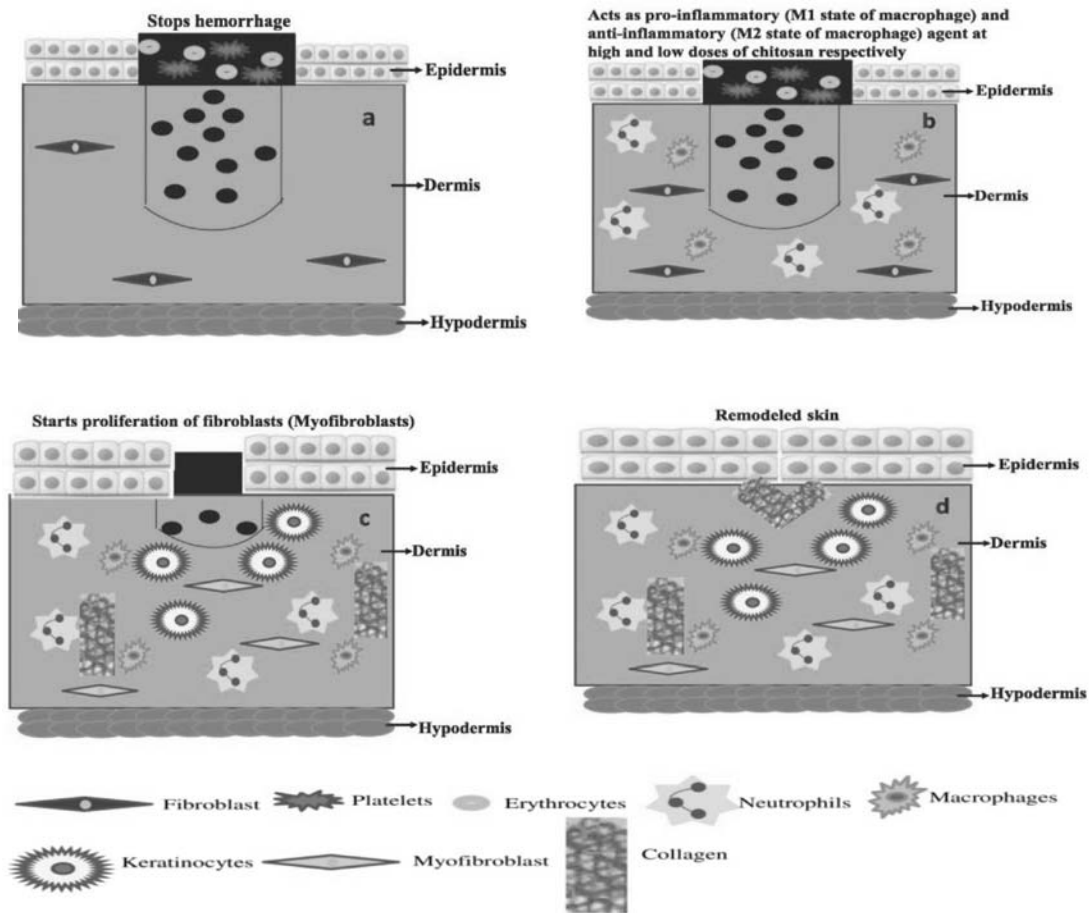


Fig. 9. Role of chitosan in different stages of wound healing

considerable antioxidant and antibacterial activity against the sixteen clinical isolates of human gram-positive and gram-negative pathogens, viz. *Bacillus cereus*, *Enterococcus* spp., *Escherichia coli*, *Klebsiella* spp., *Proteus mirabilis*, *Proteus vulgaris*, *Pseudomonas* spp., *Salmonella paratyphi A*, *Salmonella typhi*, *Salmonella typhimurium*, *Serratia* spp., *Shigella dysentery A*, *Shigella flexneri*, *Staphylococcus aureus*, *Staphylococcus epidermidis*, and *Vibrio cholera*, and the zones varied between ~12 mm and ~18.5 mm [21]. The positive charge of AgNPs enables them to anchor to the bacterial cell wall, alter the permeability of the cell membrane, and thus cause the death of cells.

Nanofibers provide a high surface area, help in efficient wound exudate absorption, and promote haemostasis - all essential for wound healing. The porosity of nanofibers helps in gaseous exchange around the wound, preventing desiccation/dehydration. Also, fibers adapt to the contour of the wound. Further, the electrospun chitosan/PVA nanofibrous scaffolds encapsulated with the AgNPs act as an interface between the AgNPs and the proliferating cells and thus protect the young cells from their toxic effects, if any, in the wound area.

5. CONCLUSION

The morphology and structure of chitosan revealed by SEM are spherical and mesoporous, and XRD analysis showed that the extracted marine chitosan is semi-crystalline and has a size of 28.9 nm. The Fourier transform infrared (FTIR) spectrum showed the occurrence of N-O, O-H, and CO stretching of bonds in the structure of chitosan. The piezoelectric property of chitosan was

determined by PFM, and the mean piezoelectric coefficient (d_{33}) was found to be 3.7 pm/V. As a natural polymer, chitosan exhibits antioxidant and hypoglycemic activities. Fabricated marine chitosan and PVA films exhibited wound healing efficacy of approximately 78% in just 8 days, when compared with control and standard. The electrospun Chitosan/PVA/AgNPs composite nanofiber showed a mean fibre diameter of 240 nm, the encapsulated AgNPs' mean particle size was about 1.31 μm and a wound efficacy of 96%. From the tensile strength characteristics of the nanofibers tested, the mean Young's modulus calculated was 215.73 MPa. Investigation of the wound healing efficiency in animal models revealed that the nanofibrous scaffold was of higher efficiency than the films in wound healing. Chitosan/PVA/AgNP composite nanofibrous wound dressings would be highly beneficial to subjects inflicted with different types of wounds and thus hold a commercial viability in the pharmaceutical market.

FUNDING

Received a seed grant from RVR & JC College of Engineering to conduct a safety and efficacy study of the fabricated wound dressing.

ACKNOWLEDGMENTS

The authors express their sincere gratitude to the Principal and the management for providing the laboratory facilities and seed grant facilitating the conduct of animal studies. The authors acknowledge Prof. CNR Research Centre, Avinashilingam Deemed University, Coimbatore and CeNS- Bangalore for FTIR, FESEM and EDS characterization. The authors

thank and acknowledge the BIO-AFM (BSBE) - IRCC BIO Atomic Force Microscopy central facility and the Department of Bio-Science & Bio-Engineering, IITB, Mumbai for the PFM facility.

Ethical approval

The protocol approved by the IAEC, Nirmala College of Pharmacy, Mangalagiri, Guntur Dt., AP, India was adopted for the animal studies (Protocol Approval number: 013/IAEC/NCPA/PhD/2019-2020).

Conflicts of interest

The authors declare no conflicts of interest.

References

1. N. P. Nirmal, C. Santivarangkna, M. S. Rajput and S. Benjakul, *Trends Food Sci. Technol.* (2020) 103:20-35.
2. S. Rubio, T. Odoom-Wubah, Q. Li, J. L. Tirado, P. Lavela, J. Huang and G. F. Ortiz, *J. Cleaner Prod.* (2022) 359:131994.
3. Y. Dong, Y. Zheng, K. Zhang, Y. Yao, L. Wang, X. Li, J. Yu and B. Ding, *Adv. Fiber Mater.* (2020) 2:212–227.
4. S. G. Jin, *Chem. - Asian J.* (2022) e202200595.
5. P. Feng, Y. Luo, C. Ke, H. Qiu, W. Wang, Y. Zhu, R. Hou, L. Xu and S. Wu, *Front. Bioeng. Biotechnol.* (2021) 9:650598.
6. S. P. Gherman, G. Biliuta, A. Bele, A. M. Ipate, R. I. Baron, L. Ochiuz, A. F. Spac and D. E. Zavastin, *Gels* (2023) 9(2):122.
7. M. Zhang, G. Wang, X. Zhang, Y. Zheng, S. Lee, D. Wang and Y. Yang, *Polymers* (2021) 13(18):3151.
8. N.M. Sachindra and N. S. Mahendrakar, *Bioresour. Technol.* (2005) 96(10):1195-1200.
9. A. Jiang, R. Patel, B. Padhan, S. Palimkar, P. Galgali, A. Adhikari, I. Varga and M. Patel, *Polymers.* (2023) 15(10):2235.
10. D. K. Maharani and W. F. R. Nurzulla, *UNESA journal of chemistry.* (2022) 11(1):61-68.
11. X. Yue, L. Liu, Y. Wu, X. Liu, S. Li, Z. Zhang, S. Han, X. Wang, Y. Chang, H. Bai, J. Chai, S. Hu and H. Wang, *Ann Transl Med.* (2021) 9(6):482.
12. A. K. Nakamura-García, E. del C. Santos-Garfias, D. I. Alonso-Martínez, T. I. Garambullo-Peña, J. F. Covián-Nares, M. Gómez-Barroso and R. Montoya-Pérez, *Revista Mexicana De Ingeniería Biomedica.* (2022) 43(1):19–31.
13. H. Chopra, S. Bibi, S. Kumar, M. S. Khan, P. Kumar and I. Singh, *Gels.* (2022) 8(2):111.
14. M. Constantin, M. Lupei, S-M. Bucatariu, I. M. Pelin, F. Doroftei, D. L. Ichim, O. M. Daraba and G. Fundueanu, *Polymers.* (2023) 15(1):4.
15. S. E. Al-Mofty, A. H. Karaly, W. A. Sarhan and H. M. E. Azzazy, *ACS Omega.*, (2022) 7(15):13210-13220.
16. D. Pradeep, G. Vishnubabu, A. Ratnakumari, B. Kumar and K. Sobha, *Res. J. Biotech.*, (2023) 18(11):40-48.
17. C. Y. Hsu, Y. P. Chan and J. Chang, *Biol. Res.*, (2007) 40:13-21.
18. A. A. Adedapo, F. O. Jimoh, S. Koduru, P. J. Masika and A. J. Afolayan, *BMC Complement Altern Med.*, (2009) 9(1):1-8.
19. M Oyaizu, *Japanese Journal of Nutrition.*, (1986) 44(6):307-315.
20. P. Bernfeld, *Methods in Enzymology.* (1955) 1:149-158.
21. K. Sobha, D. Pradeep, A. Ratna Kumari, V. Mahendra Kumar and K. Surendranath, *Sci Rep.*, (2017) 7:11566.
22. M. Shahla, T. Shiva, A. A. Kofi and N. Ali, *AAPS Pharm Sci Tech*, (2021) 22: 170

Chitosan/PVA Films and Silver Nanoparticle Impregnated Nanofibrous Dressings for 303
Evaluation of their Wound Healing Efficacy in Wistar Albino Rat Model

23. V. Balan, C. T. Mihai, F. D. Cojocaru, C. M. Uritu, G. Dodi, D. Botezat and I. Gardikiotis, *Materials*, (2019) 12(18): 2884.
24. M. B. Povea, W. A. Monal, J. V. Cauich-Rodríguez, A. M. Pat, N. B. Rivero and C. P. Covas, *Mater. Sci. Appl.*, (2011) 2(6): 509-520.
25. M. Kaya, O. Seyyar, T. Baran, T. Turkes, *Front. Zool.*, (2014) 11(1):1-10
26. S. Kumari, P. Rath and A. Sri hari kumar, *Afr. J. Biotechnol.*, (2006) 15(24):1258-1268.
27. S. Maya, S. Vijay, M. Giridhar and B. Suryasarathi, *RSC Adv.*, (2016) 6: 6251-6258.
28. G. Amanuel, M. Giridhar, and B. Suryasarathi, *ACS Omega*, (2018) 3: 5317-5326.
29. S. Sawan, A. M. Shanmugaraj and S. Anandhan, *Journal of Polymer Research*, (2021) 28:419.
30. N. More and G. Kapusetti, *Medical Hypotheses*, (2017) 108:10-16.
31. T. Sun, D. Zhou, F. Mao and Y. Zhu, *Eur. Polym. J.*, (2007) 43(2):652-656.
32. T. N. Tran, C. T. Doan, V. B. Nguyen, A. D. Nguyen and S. L. Wang, *Polymers (Basel)*., (2019) 11(10):1714.
33. J. Liu, J. F. Lu, J. Kan, Y. Q. Tang and C. H. Jin, *Int. J. Biol. Macromol.*, (2013) 62:85-93.
34. D. S. Lee, J. Y. Woo, C. B. Ahn and J. Y. Je, *Food Chem.*, (2014) 148:97-104.
35. M. S. R. Rajoka, L. Zhao, H. M. Mehwish, Y. Wu and S. Mahmood, *Appl. Microbiol. Biotechnol.* (2019) 103:1557-1571.
36. V. Poitout and R. P. Robertson, *Endocr Rev.* (2008) 29(3):351-366.
37. F. Karadeniz, M. Artan, C. S. Kong and S. K. Kim, *Carbohydr. Polym.* (2010) 82(1):143-147.
38. M. Abbas, T. Hussain, M. Arshad and A. R. Ansari, *Int. J. Biol. Macromol.*, (2019) 140:871-876.
39. D. Fong and C. D. Hoemann, *Future Sci OA.*, (2017) 4(1):FSO225.

Received: 26-08-2023

Accepted: 11-11-2023